

DFT study of migration enthalpies in MgSiO₃ perovskite

M. W. Ammann · J. P. Brodholt · D. P. Dobson

Received: 28 March 2008 / Accepted: 7 September 2008 / Published online: 23 September 2008
© Springer-Verlag 2008

Abstract The effect of pressure on ionic diffusion in orthorhombic MgSiO₃ perovskite has been investigated using density functional theory. An intensive investigation of possible silicon pathways revealed new positions of the saddle-points and an enthalpy of migration at 26.2 GPa of 4.7 eV that is in fair agreement with the experimental values of about 3.5 eV at 25 GPa. This is much lower than found in previous studies (~9 eV) and removes the need to explain silicon diffusion by a complicated process involving coupled oxygen vacancies, as has been previously proposed. Our migration enthalpies for oxygen and magnesium are in excellent agreement with experiments. We find that oxygen diffusion occurs via a chain of several inequivalent jumps along the octahedron edges, and that magnesium occurs via two inequivalent [110] jumps and one [001] jump. We also present activation volumes for all three species at 25 and 135 GPa.

Keywords Migration enthalpies · MgSiO₃ perovskite · High pressure · Rheology of lower mantle

Introduction

An accurate knowledge of the transport properties of Earth's mantle is necessary for modelling its thermochemical evolution and understanding its present state (Dobson and Brodholt 2000). The rheology, reaction rates and (ionic) electrical conductivity of mantle minerals are all ultimately controlled by the chemical diffusivities of

their constituent chemical species. Magnesium silicate, MgSiO₃, perovskite is the volumetrically dominant mineral in the mantle, comprising some 70–80% of the lower mantle and the change in viscosity at 670 km depth is thought to exert a fundamental control on mantle convection (Hager 1984). Despite its importance, however, chemical diffusivity in silicate perovskite is poorly understood. There are very few experimental studies of diffusion in perovskite and only at the pressures of the uppermost few kilometers of the lower mantle. Furthermore, previous numerical simulation studies (Karki and Khanduja 2007; Wright and Price 1993) could not reproduce the experimental values for silicon migration enthalpy and disagree in the migration direction of magnesium. Here we present an ab initio simulation study of the migration enthalpies of magnesium, silicon and oxygen in MgSiO₃ perovskite at various pressures throughout the Earth's mantle. The migration enthalpies determined here agree well with experimentally determined values for all three species.

Methodology

Calculations were performed using the ab initio total-energy calculation package VASP (Vienna ab initio Simulation Package) (Kresse and Hafner 1993; Kresse and Furthmüller 1996) which uses density functional theory (Hohenberg and Kohn 1964; Kohn and Sham 1965). The Generalised Gradient Approximation (Perdew and Wang 1992) and the projector augmented-wave method (Blöchl 1994; Kresse and Joubert 1999) were used. Pressure was imposed by a constant volume approach as suggested by Karki and Khanduja (2006). All calculations have been performed in a static, fully relaxed crystal. A 2 × 2 × 2-supercell of orthorhombic MgSiO₃ perovskite

M. W. Ammann (✉) · J. P. Brodholt · D. P. Dobson
Department of Earth Sciences, University College London,
Gower Street, London WC1E 6BT, UK
e-mail: m.ammann@ucl.ac.uk

in the Pbnm space group was used containing 160 atoms. Migrations enthalpies calculated with the $2 \times 2 \times 2$ cell agree to within 0.05 eV with those calculated using a smaller $2 \times 2 \times 1$ cell; the $2 \times 2 \times 2$ cell is, therefore, sufficiently large. All calculations have been performed using a single k-point (Γ -point) sampling. The comparison with a $4 \times 4 \times 4$ -k-point sampling revealed a difference in the migration enthalpy of less than 0.2%. A plane wave basis-set expansion with a cut-off energy of 1000 eV was used for the representation of the valence electrons. Compared with a cut-off energy of 1200 eV, migration enthalpies changed by less than 0.1%.

Migration enthalpies

Atomic migration is considered as a hopping process: an ion moves from one site into a nearby vacancy. In this work we are only considering the ionic defects and remove either an Mg^{2+} , Si^{4+} or O^{2-} in each calculation. The net charges of the magnesium, silicon and oxygen vacancies are, therefore, -2 , -4 and $+2$, respectively, which are considered the dominant defect in silicates (Karki and Khanduja 2007; Wright and Price 1993). Generally, the computation of the energies of charged systems using periodic boundary conditions requires a correction for the self-interaction with the system's images (Brodholt 1997). However, as only energy differences were considered in this study, no such correction needed to be applied as the corrections cancel each other. During migration of a single ion, it needs to overcome the potential energy barrier which it crosses at a saddle-point where it has the highest energy. In the activated state, the diffusing ion sits at the top of the

saddle-point, in an interstitial site, with two near-neighbour vacancies, one on the site which the ion has vacated and one on the site which the ion is migrating to. The migration enthalpy of an ion is then defined as the energy difference between the equilibrium defective system and the defective system with an ion at the saddle-point:

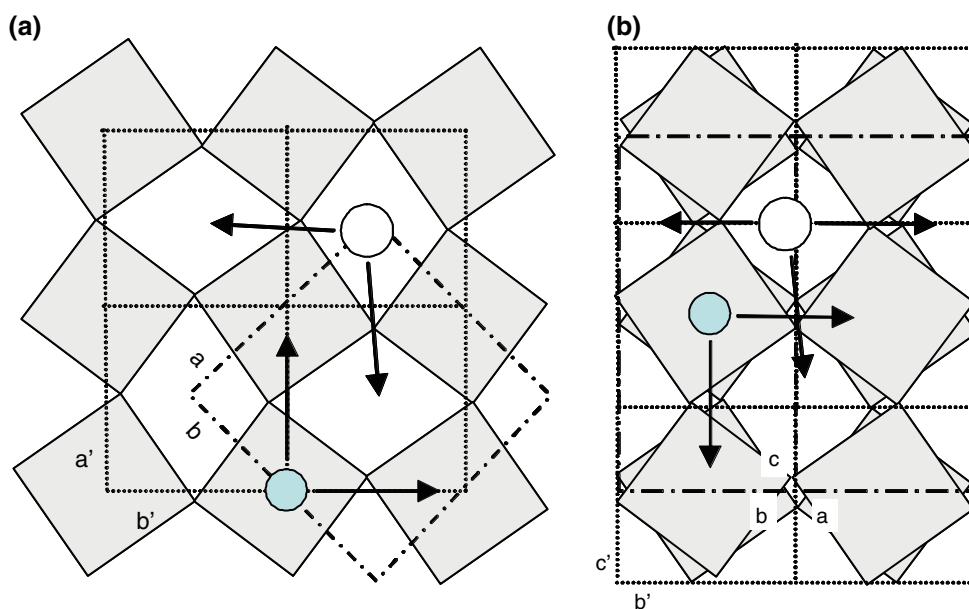
$$E_{\text{migration}} = E_{\text{saddlepoint}} - E_{\text{equilibrium}}$$

Although the saddle-point lies approximately halfway between the occupied and vacant site, as stated by Wright and Price (1993), finding the exact location is not always straightforward. We have, therefore, spent considerable effort in locating the saddle-point, as described below. This is particularly important for silicon migration.

Perovskite structure

Magnesium silicate perovskite is distorted from the cubic type-structure by tilting of the SiO_6 octahedra as sketched in Fig. 1. The distortion results in a rotation of the a - and b -axes by 45° from the cubic structure with a consequent increase of the axial lengths of approximately $\sqrt{2}$. The orthorhombic c -axis is doubled from the cubic axis, resulting in four formula units in the unit cell for the orthorhombic structure. Silicon and magnesium nearest neighbours, and hence shortest hopping distances, lie along the axial vectors in the pseudo-cubic setting and along $[110]$ and $[001]$ in the orthorhombic setting (Fig. 1). In the present study we consider the jumps to nearest neighbours (i.e. along $[110]$) as well as jumps to next-nearest neighbours in the x - y plane (i.e. along $[100]$ and $[010]$). Furthermore, silicon lies on $(1/2, 0, 1/2)$ such that $[110]$ and $[-110]$ jumps are equivalent. For magnesium, in contrast,

Fig. 1 Sketch of the magnesium silicate structure. **a** View down c -axis; **b** projection onto (110) of the orthorhombic cell. For clarity oxygen atoms have been omitted and the SiO_6 octahedra are indicated in grey. The pseudocubic unit cell is shown using dotted lines and the orthorhombic cell is shown in dot-dashed lines; pseudocubic (orthorhombic) axes are labelled with (without) a tick. One silicon atom (small green) and one magnesium atom (large white) are shown along with their nearest neighbour jumps (arrows)



they are not equivalent as the positions of the ions near the paths are different due to the tilt of the SiO_6 octahedra (see also Fig. 4), giving two possible diagonal migration pathways. For oxygen we have considered all of the possible exchanges along the octahedron edges as well as the two inequivalent next-nearest neighbour jumps along [001] (see below).

Silicon migration

The silicon migration pathways are complex and a geometrical analysis yields only a vague indication of the saddle-point's position: in order to avoid the obstructing oxygens, the migrating silicon ion passes approximately half-way between all the oxygen and magnesium ions. The situation is shown in Fig. 2. Assuming that the saddle-point lies halfway between the vacant and the jumping ion's site, one needs to search in a plane of possible saddle-points half-way between the two sites. For the [110]-pathway, the initial and final sites are respectively $(1/2, 1/4, 1/2)$ and $(1/4, 1/2, 1/2)$ in relative coordinates within the $2 \times 2 \times 2$ -supercell. The condition $x = y$ defines the saddle-point plane, and we searched within that plane for the minimum energy. For the [001]-pathway, the initial and final sites are respectively $(1/2, 1/4, 1/4)$ and $(1/2, 1/4, 1/2)$, where the condition $z = 3/8$ defines the saddle-point plane within which we search. For the second nearest neighbour jumps, i.e. along [100] and [010], we again assume that the saddle-point plane is exactly half-way between the two sites. However, we find that these jumps are always energetically very unfavourable compared with the nearest neighbour

jumps (see Table 1) and so we have not searched the entire saddle-point plane.

By sampling the plane at many different points, the minimum energy location in the plane of possible saddle-points was found to be $z = 0.44$ and $x = y = 0.37$ with respect to the supercell for the [110]-pathway and $x = 0.6$, $y = 0.33$ and $z = 0.375$ for the [001]-pathway. Figure 3 shows contour maps of saddle-point energies (migration enthalpies) created by cubic interpolation between the sampling points in the plane of possible saddle-points on the [110]-pathway at 3.3 and 151.7 GPa. The minimum for the pathway along the [001]-direction is not particularly strong and therefore no map is shown. A comparison of the two contour maps at 3.3 and 151.7 GPa shown in Fig. 3 reveals a small change in the topology of the energy surface in the plane of possible saddle-points with pressure: with increasing pressure, the high energy plateaus surrounding the oxygen (upper right corner) and the magnesium (lower left corner) are pushed closer together resulting in two possible pathways for the migrating silicon. One passes underneath the oxygen, the other one avoids it by going around it on its left side. Both pathways are marked with their corresponding migration enthalpy in Fig. 3. The location of the minimum migration enthalpy for both pathways does not change between the 3.3 GPa and 151.7 GPa simulations and we thus assumed that the location of the saddle-point remains at the same relative position at all pressures. The maps also clearly demonstrate how choosing the saddle-point position in different regions can result in much too high migration enthalpies explaining findings of previous studies. Furthermore, the calculated migration enthalpies

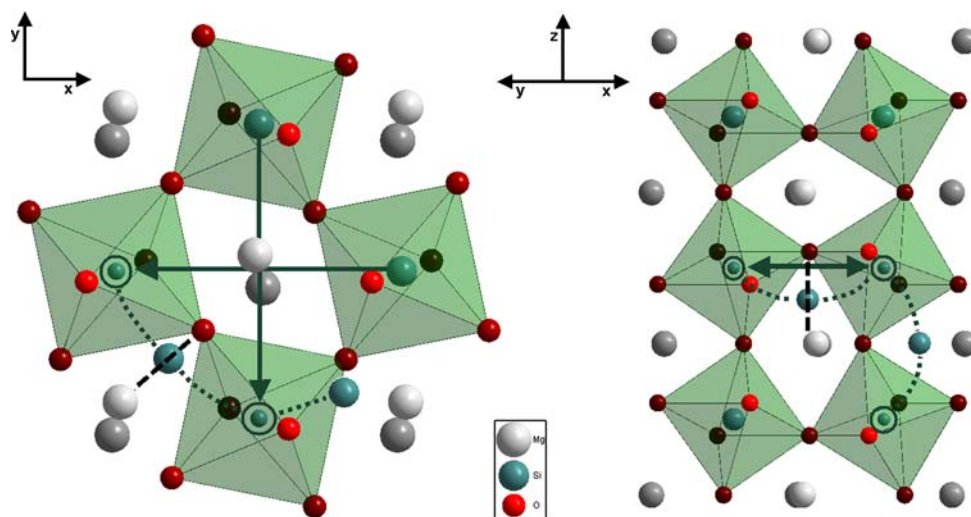


Fig. 2 Sketch of silicon migration pathways in orthorhombic MgSiO_3 perovskite [*left* view in z -direction, *right* projection onto (110)]. *Straight-line* pathways are indicated as *solid arrows* and are much higher energy than the curved pathways (see Table 1). In the right hand side figure, the *straight-line* pathways have a component

out of the paper. *Darker* atoms are farther away from the observer. On the curved pathways, the migrating silicon is positioned at the saddle-point location. Vacancy sites are indicated with *circles* and the plane of possible saddle-points is shown by *dashed lines*

Table 1 Migration enthalpies (in eV) of silicon in orthorhombic MgSiO₃ perovskite for different migration pathways at different pressures (in GPa)

	Pathway	3.3 GPa	26.2 GPa	61.0 GPa	101.1 GPa	126.6 GPa	151.7 GPa
This Study	[110]	3.52	4.7	5.6	6.17	6.41	6.59
	[100]	6.98	–	–	–	–	–
	[010]	7.95	–	–	–	–	–
	[001]	5.72	–	–	–	8.25	–
Karki and Khanduja (2007)	[110]	8.33 ^a	9.1 ^b	~9.7	~10.2	10.48 ^c	~10.8
	[001]	19.56 ^a	–	–	–	–	–
Wright and Price (1993)	[110]	9.2 ^a	–	–	–	10.32 ^d	–
Dobson et al. (2008)	Exp.	–	3.6 ± 0.76 ^e	–	–	–	–
Yamazaki et al. (2000)	Exp.	–	3.48 ± 0.38 ^e	–	–	–	–

The “~” symbol indicates that the numbers were read out of figures

^a At 0 GPa

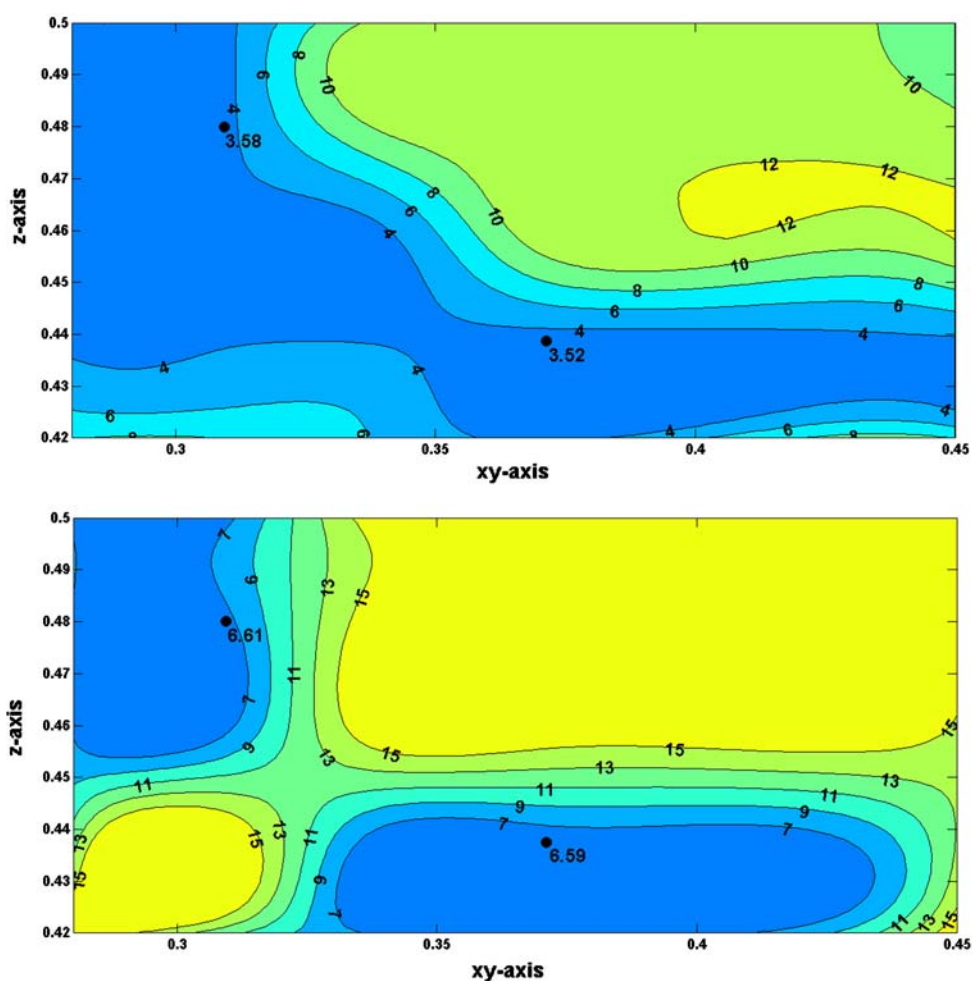
^b At 30 GPa

^c At 120 GPa

^d At 125 GPa

^e At 25 GPa

Fig. 3 Contour maps of the computed migration enthalpies (in eV) in the sampled plane of possible saddle-points for silicon migration along the [110]-pathway in orthorhombic MgSiO₃ perovskite at 3.3 GPa (*upper*) and at 151.7 GPa (*lower*). The locations of the minimum of migration enthalpy for two possible silicon pathways are marked with a *black dot* and labelled with their corresponding value



can depend on the initial crystal structure since the energy surface of the activated state contains many local minima. Thus, if the system is allowed to relax from an initial configuration of an interstitial silicon placed in the perfect structure (with vacancies placed on the starting and final silicon-sites of the migration pathway) it finds a minimum energy which is ~ 5 eV higher than if the initial configuration uses a structure which has been relaxed around a vacancy on the target site. This suggests that only a local minimum is found when one starts the structural optimisation from the perfect structure, and highlights the difficulty in finding global minima. The agreement between our results and experiments, shown below, suggests that we must be close to the global minimum. Finally we tested whether the saddle-point is in a local minimum of the migration path by moving the ion a small distance off the plane towards a vacancy and confirming the energy decreased.

The silicon migration enthalpies for different directions at a range of pressures are shown in Table 1. Each jump between nearest neighbours in any direction in the x - y -plane is equivalent and only two jumps are required to cross a unit cell. The [100] and [010] migration pathways which constitute direct jumps across one unit cell to the second nearest neighbours (solid lines in Fig. 1) are energetically unfavourable. The high migration enthalpy in the [001]-direction (Table 1) is in agreement with anisotropic silicon-diffusion seen in experimental data (Dobson et al. 2008). A comparison between the silicon migration enthalpy at 26.2 GPa of 4.7 eV and its experimental values of 3.6 ± 0.76 eV (Dobson et al. 2008) and 3.48 ± 0.38 eV (Yamazaki et al. 2000) at 25 GPa shows the best agreement found so far in any theoretical study.

The migration enthalpies increase with pressure as expected from the decreased inter-atomic distances in the compressed structures. The activation volume decreases from $3.5 \text{ cm}^3/\text{mol}$ at 25 GPa to $0.7 \text{ cm}^3/\text{mol}$ at 135 GPa.

Magnesium migration

There are three distinct pathways to nearest neighbour sites for magnesium as shown in Fig. 4. Pathways to second nearest neighbours around the octahedra (between oxygen and magnesium) along [100] and [010] are energetically unfavourable (as shown in Table 2). The two [110]-pathways (*a* and *b*) pass between two octahedra and are strongly affected by nearby oxygens, and so one cannot assume a straight-line path. For path *b* a migration enthalpy of 2.52 eV is found for a magnesium ion passing halfway between the initial and final ion site and halfway between the nearest oxygen neighbours (as shown in Fig. 4), whereas a straight-line between the two magnesium yields a much higher migration enthalpy of 13.5 eV. Shifting the ion off the straight-line path is less important for pathway *a* with the migration enthalpy changing from 3.3 to 3.1 eV by shifting off the straight-line path. Similarly, the straight-line path in the [001]-direction passes halfway between pairs of oxygens and yields a saddle-point halfway between the initial and final sites. The positions of the saddle-points have been re-calculated for each pressure as the local ionic structure changes slightly with increasing pressure. As in the case of silicon migration, it is unlikely that the saddle-point has been found exactly and as such all migration enthalpies are, within errors, approximately equal to each other and to the experimental value. Moreover, the results show that diffusion of magnesium is isotropic.

The computed magnesium migration enthalpies for different directions and pressures are shown in Table 2. The average magnesium migration enthalpy at 26.2 GPa of 3.69 ± 0.37 eV is somewhat smaller than the experimental value for Fe–Mg-interdiffusion of 4.29 ± 0.64 eV at 24 GPa (Holzapfel et al. 2005). However, as the locations of the chosen saddle-points do not correspond exactly with the real saddle-points, it is possible that they lie close to the

Fig. 4 Sketch of magnesium migration pathways in orthorhombic MgSiO_3 perovskite [*left* view in z -direction, *right* projection onto (110)]. Straight-line pathways are indicated as solid arrows. Darker atoms are farther away from the observer. On the curved pathways, the migrating magnesium is positioned at the saddle-point location (only in the left figure). Vacancy locations are indicated with circles

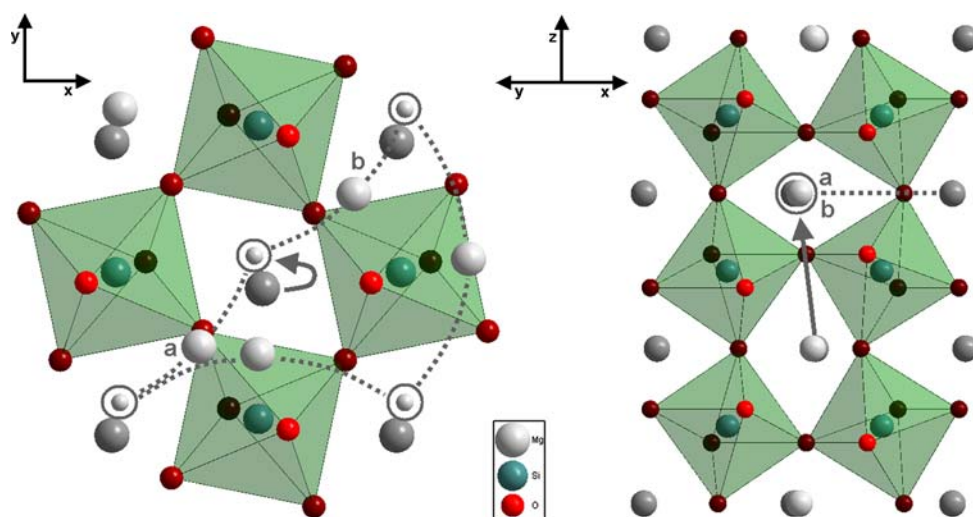


Table 2 Migration enthalpies (in eV) of magnesium in orthorhombic MgSiO₃ perovskite for different migration pathways at different pressures (in GPa)

	Pathway	3.3 GPa	26.2 GPa	61.0 GPa	101.1 GPa	126.6 GPa	151.7 GPa
This Study	[110] a	3.1	3.96	5.21	5.7	6.2	6.71
	[110] b	2.52	3.27	4.35	5.12	5.55	6.15
	[001]	2.87	3.84	4.82	5.74	6.21	6.73
	Average	2.83 ± 0.29	3.69 ± 0.37	4.79 ± 0.43	5.52 ± 0.34	5.98 ± 0.38	6.53 ± 0.33
	[100]	7.74	–	–	–	–	–
	[010]	9.07	–	–	–	–	–
Karki and Khanduja (2007)	[110]	3.47 ^a	4.78 ^b	~6.1	~7	7.71 ^c	~8.7
	[001]	13.54 ^a	–	–	–	–	–
Wright and Price (1993)	[110]	4.57 ^a	–	6.13 ^d	–	7.43 ^e	–
Holzappel et al. (2005)	Exp.	–	4.29 ± 0.64 ^f	–	–	–	–

The “~” symbol indicates that the numbers were read out of figures

^a At 0 GPa

^b At 30 GPa

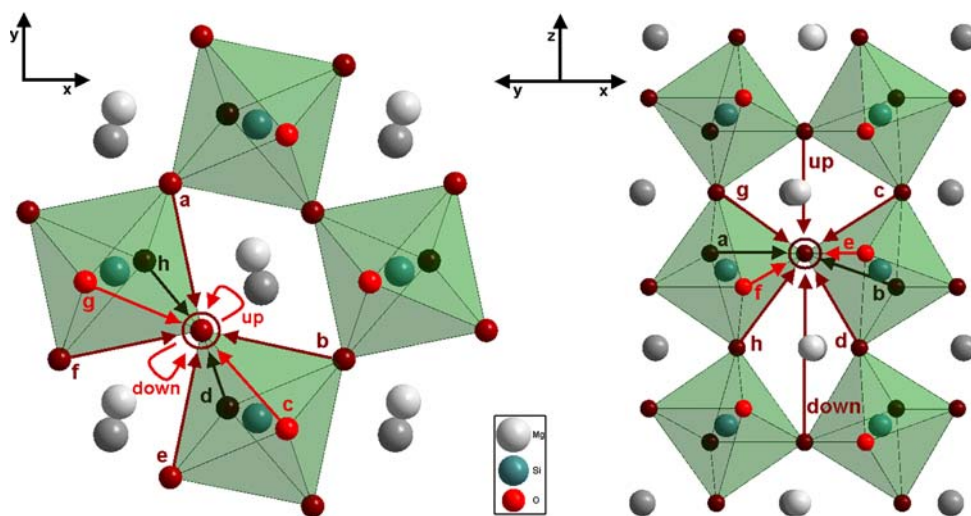
^c At 120 GPa

^d At 60 GPa

^e At 125 GPa

^f Fe-Mg inter-diffusion at 24 GPa

Fig. 5 Sketch of oxygen migration pathways in orthorhombic MgSiO₃ perovskite [*left* view in *z*-direction, *right* projection onto (110)]. *Straight-line* pathways are indicated as *solid arrows*. *Darker* atoms are farther away from the observer. The vacancy location is indicated with a *circle*



correct path resulting in lower migration enthalpies. Additionally, one can expect a lower enthalpy for pure magnesium migration, as observed here, since iron is larger than magnesium resulting in a stronger lattice distortion at the saddle-point and increased migration enthalpies. Thus, the present values are consistent with experiment. The activation volumes calculated from the average values at 25 GPa is 3.37 cm³/mol and at 135 GPa 2.05 cm³/mol.

Oxygen migration

Oxygen migration can take place along many distinct pathways as shown in Fig. 5. Although there are only two

inequivalent oxygen positions within the unit cell, there are eight different (non-equivalent) jumps that an oxygen can perform along octahedra edges.

The migration enthalpies were calculated by setting an oxygen exactly halfway between the initial and end sites. Again, the saddle-point may not lie exactly halfway between two oxygen sites, but as all migration enthalpies are equal to the experimental value within error, the mid-way position must be close to the true saddle-point. These are shown in Table 3. Note that the eight different jumps along the edges of the octahedra have similar migration enthalpies; this is to be expected since the octahedral distortions are small. The average oxygen migration enthalpy

Table 3 Migration enthalpies (in eV) of oxygen in orthorhombic MgSiO₃ perovskite for different migration pathways at different pressures (in GPa)

	Pathway	3.3 GPa	26.2 GPa	61.0 GPa	101.1 GPa	126.6 GPa	151.7 GPa
This Study	[001] Up	2.9	2.99	–	–	–	3.29
	[001] Down	10.71	–	–	–	–	–
	a	0.72	1.5	2.11	2.75	2.89	2.87
	b	0.8	1.78	2.24	2.88	2.91	3.05
	c	1.29	1.16	1.94	2.38	1.58	2.08
	d	0.92	0.97	1.24	2.26	2.65	2.96
	e	0.55	1.5	1.79	2.38	2.73	3.31
	f	0.86	1.63	2.56	2.78	2.76	3.51
	g	0.66	1.42	1.74	2.2	2.61	3.22
	h	0.97	1.8	2.17	2.52	2.9	3.07
	Average	0.85 ± 0.23	1.47 ± 0.29	1.97 ± 0.4	2.53 ± 0.26	2.63 ± 0.44	3.01 ± 0.43
Karki and Khanduja (2007)	[100]	0.57 ^a	1.41 ^b	~2	~2.5	2.57 ^c	~2.5
	[110]	2.78 ^a	–	–	–	–	–
Wright and Price (1993)	[100]	0.96 ^a	–	–	–	–	–
Dobson (2003)	Exp.	–	1.35 ± 0.2 ^d	–	–	–	–
Xu and McCammon (2002)	Exp.	–	1.47 ^d	–	–	–	–

The definition of the pathways and their labels are given in Fig. 5. The average values are given with their standard deviations. The “~” symbol indicates that the numbers were read out of figures

^a At 0 GPa

^b At 30 GPa

^c At 120 GPa

^d At 25 GPa

at 26.2 GPa of 1.47 eV is in excellent agreement with the experimental value of 1.35 eV (Dobson 2003) or 1.47 eV (Xu and McCammon 2002) at 25 GPa. The activation volume calculated from the average values at 25 GPa is 1.95 cm³/mol, and decreases to 1.49 cm³/mol at 135 GPa. The high migration enthalpies for the pathways up and down clearly demonstrate that migration takes place along the octahedra edges. The similar migration enthalpies along octahedra edges means that oxygen diffusion in perovskite is essentially isotropic.

Discussion

First-principles simulations of orthorhombic MgSiO₃ perovskite have been performed in order to compute the migration enthalpies of magnesium, silicon and oxygen under different pressures up to lower mantle conditions. All migration enthalpies increase monotonically with increasing pressure. Our results agree well with experimental results. A new silicon migration pathway has been proposed yielding a migration enthalpy much closer to the experimental value than in previous studies (Karki and Khanduja 2007; Wright and Price 1993). We suggest, therefore, that silicon diffuses via a simple hopping

mechanism and does not require a complicated process involving adjacent oxygen vacancies, as suggested by the previous studies.

The rate of deformation in high-temperature dislocation-migration regimes is limited by the slowest diffusing species. Our calculated migration enthalpies for silicon diffusion are about 20% higher than magnesium at all pressures, and substantially higher than oxygen. This suggests that silicon will be the rate-limiting species throughout the Earth's mantle, as is the case with most silicates (Dobson et al. 2008). Recent experiments (Holzapfel et al. 2005; Dobson et al. 2008) suggest that silicon and magnesium have very similar diffusivities such that silicon is not necessarily the rate-limiting species. However, the experiments of (Holzapfel et al. 2005) are Fe–Mg inter-diffusion and so the migration enthalpy they measure may well be higher than that for magnesium self-diffusion. Furthermore, the formation energy of silicon vacancies is generally significantly higher than for magnesium or oxygen vacancies (e.g. Brodholt 1997).

Holzapfel et al. (2005) extrapolate their Fe–Mg inter-diffusion values to deep lower mantle conditions using a constant activation volume of 2.1 cm³/mol from Wright and Price (1993). This activation volume is equal (within error) to those found in this study and we do not find a

strong pressure dependence of activation volume for magnesium migration. The conclusions of Holzapfel et al. (2005) are therefore not affected by the present study. In contrast, the extrapolation by Xu and McCammon (2002) will underestimate oxygen mobility at the base of the lower mantle since they use an activation volume of about $2.1 \text{ cm}^3/\text{mol}$, which is somewhat larger than the value found here at high pressure. This makes it even more likely that oxygen ionic conduction in MgSiO_3 occurs towards the base of the lower mantle.

Acknowledgments This work was funded by the European Commission through the Marie Curie Research Training Network “c2c” Contract No. MRTN-CT-2006-035957. This work made use of the facilities of HECToR, the UK’s national high-performance computing service, which is provided by UoE HPCx Ltd at the University of Edinburgh, Cray Inc and NAG Ltd, and funded by the Office of Science and Technology through EPSRC’s High End Computing Programme.

References

- Blöchl PE (1994) Projector augmented-wave method. *Phys Rev B* 50:17953–17979. doi:[10.1103/PhysRevB.50.17953](https://doi.org/10.1103/PhysRevB.50.17953)
- Brodholt JP (1997) Ab initio calculations on point defects in forsterite (Mg_2SiO_4) and implications for diffusion creep. *Am Mineral* 82:1049–1053
- Dobson DP (2003) Oxygen ionic conduction in MgSiO_3 perovskite. *Phys Earth Planet Inter* 139:55–64. doi:[10.1016/S0031-9201\(03\)00144-4](https://doi.org/10.1016/S0031-9201(03)00144-4)
- Dobson DP, Brodholt JP (2000) The electrical conductivity and thermal profile of the earth’s mid-mantle. *Geophys Res Lett* 27:2325–2328. doi:[10.1029/1999GL008409](https://doi.org/10.1029/1999GL008409)
- Dobson DP, Dohmen R, Wiedenbeck M (2008) Self-diffusion of oxygen and silicon in MgSiO_3 perovskite. *Earth Planet Sci Lett* 270:125–129. doi:[10.1016/j.epsl.2008.03.029](https://doi.org/10.1016/j.epsl.2008.03.029)
- Hager BH (1984) Subducted slabs and the geoid: constraints on mantle rheology and flow. *J Geophys Res* 89:6003–6015. doi:[10.1029/JB089iB07p06003](https://doi.org/10.1029/JB089iB07p06003)
- Hohenberg P, Kohn W (1964) Inhomogeneous electron gas. *Phys Rev* 136:B864–B871. doi:[10.1103/PhysRev.136.B864](https://doi.org/10.1103/PhysRev.136.B864)
- Holzapfel C, Rubie DC, Frost DJ, Langenhorst F (2005) Fe–Mg interdiffusion in $(\text{Mg}; \text{Fe})\text{SiO}_3$ perovskite and lower mantle reequilibration. *Science* 309:1707–1710. doi:[10.1126/science.1111895](https://doi.org/10.1126/science.1111895)
- Karki BB, Khanduja G (2006) Vacancy defects in MgO at high pressure. *Am Mineral* 91:511–516. doi:[10.2138/am.2006.1998](https://doi.org/10.2138/am.2006.1998)
- Karki BB, Khanduja G (2007) A computational study of ionic vacancies and diffusion in MgSiO_3 perovskite and post-perovskite. *Earth Planet Sci Lett* 260:201–211. doi:[10.1016/j.epsl.2007.05.031](https://doi.org/10.1016/j.epsl.2007.05.031)
- Kohn W, Sham LJ (1965) Self-consistent equations including exchange and correlation effects. *Phys Rev* 140:A1133–A1138. doi:[10.1103/PhysRev.140.A1133](https://doi.org/10.1103/PhysRev.140.A1133)
- Kresse G, Hafner J (1993) Ab initio molecular dynamics for liquid metals. *Phys Rev B* 47:558–561. doi:[10.1103/PhysRevB.47.558](https://doi.org/10.1103/PhysRevB.47.558)
- Kresse G, Furthmüller J (1996) Efficiency of ab-initio total energy calculations for metals and semiconductors using a plane-wave basis set. *Comput Mat Sci* 6:15–50. doi:[10.1016/0927-0256\(96\)00008-0](https://doi.org/10.1016/0927-0256(96)00008-0)
- Kresse G, Joubert J (1999) From ultrasoft pseudopotentials to the projector augmented wave method. *Phys Rev B* 59:1758–1775. doi:[10.1103/PhysRevB.59.1758](https://doi.org/10.1103/PhysRevB.59.1758)
- Perdew JP, Wang Y (1992) Accurate and simple analytic representation of the electron-gas correlation energy. *Phys Rev B* 45:13244–13249. doi:[10.1103/PhysRevB.45.13244](https://doi.org/10.1103/PhysRevB.45.13244)
- Wright K, Price GD (1993) Computer simulation of defects and diffusion in perovskite. *J Geophys Res* 98:22.245–22.253
- Yamazaki D, Kato T, Yurimoto H, Ohtani E, Toriumi M (2000) Silicon self-diffusion in MgSiO_3 perovskite at 25 GPa. *Phys Earth Planet Inter* 119:299–309. doi:[10.1016/S0031-9201\(00\)00135-7](https://doi.org/10.1016/S0031-9201(00)00135-7)
- Xu Y, McCammon C (2002) Evidence for ionic conductivity in lower mantle $(\text{Mg}, \text{Fe})(\text{Si}, \text{Al})\text{O}_3$ perovskite. *J Geophys Res* 107. doi:[10.1029/2001JB000677](https://doi.org/10.1029/2001JB000677)